Frontiers of Physics
https://doi.org/10.1007/s11467-019-0946-8
Front. Phys.
15(2), 24601 (2020)

RESEARCH ARTICLE

Implications on the origin of cosmic rays in light of 10 TV spectral softenings

Chuan Yue[1], Peng-Xiong Ma[1,2], Qiang Yuan[1,2,3,†], Yi-Zhong Fan[1,2,‡], Zhan-Fang Chen[1,2], Ming-Yang Cui[1], Hao-Ting Dai[4], Tie-Kuang Dong[1], Xiaoyuan Huang[1], Wei Jiang[1,2], Shi-Jun Lei[1], Xiang Li[1], Cheng-Ming Liu[4], Hao Liu[1], Yang Liu[1], Chuan-Ning Luo[1,2], Xu Pan[1,2], Wen-Xi Peng[5], Rui Qiao[5], Yi-Feng Wei[4], Li-Bo Wu[4], Zhi-Hui Xu[1,2], Zun-Lei Xu[1], Guan-Wen Yuan[1,2], Jing-Jing Zang[1], Ya-Peng Zhang[6], Yong-Jie Zhang[6], Yun-Long Zhang[4]

[1] *Key Laboratory of Dark Matter and Space Astronomy, Purple Mountain Observatory, Chinese Academy of Sciences, Nanjing 210033, China*
[2] *School of Astronomy and Space Science, University of Science and Technology of China, Hefei 230026, China*
[3] *Center for High Energy Physics, Peking University, Beijing 100871, China*
[4] *State Key Laboratory of Particle Detection and Electronics, University of Science and Technology of China, Hefei 230026, China*
[5] *Key Laboratory of Particle Astrophysics, Institute of High Energy Physics, Chinese Academy of Sciences, Beijing 100049, China*
[6] *Institute of Modern Physics, Chinese Academy of Sciences, Lanzhou 730000, China*
Corresponding authors. E-mail: [†]*yuanq@pmo.ac.cn,* [‡]*yzfan@pmo.ac.cn*
Received October 3, 2019; accepted November 28, 2019

Precise measurements of the energy spectra of cosmic rays (CRs) show various kinds of features deviating from single power-laws, which give very interesting and important implications on their origin and propagation. Previous measurements from a few balloon and space experiments indicate the existence of spectral softenings around 10 TV for protons (and probably also for Helium nuclei). Very recently, the DArk Matter Particle Explorer (DAMPE) measurement about the proton spectrum clearly reveals such a softening with a high significance. Here we study the implications of these new measurements, as well as the groundbased indirect measurements, on the origin of CRs. We find that a single component of CRs fails to fit the spectral softening and the air shower experiment data simultaneously. In the framework of multiple components, we discuss two possible scenarios, the multiple source population scenario and the background plus nearby source scenario. Both scenarios give reasonable fits to the wide-band data from TeV to 100 PeV energies. Considering the anisotropy observations, the nearby source model is favored.

Keywords cosmic rays

1 Introduction

The origin of cosmic rays (CRs) remains an unresolved question after more than one century since their discovery. To identify the sources of CRs is difficult due to that the diffusive propagation of charged particles in the random magnetic field results in the loss of the original directions of CRs. Precise measurements of the energy spectra of various species of CRs are helpful in understanding their origin and propogation. The energy spectra of CRs from the acceleration sources are generally believed to be power-laws with cutoffs due to the maximum acceleration limits of specific types of sources. The diffusion in the Galaxy results in softenings of the accelerated spectra, by a power-law of $E^{-\delta}$, which reflects the energy-dependence of the diffusion coefficient and hence the turbulent properties of the interstellar medium. Such an effect has been supported by the measurement of the secondary-to-primary flux ratios of CR nuclei [1].

However, several balloon and space experiments revealed remarkable spectral hardenings of CR nuclei around a few hundred GV rigidities [2–8]. These results inspire quite a number of discussions of their possible implications on the origin [9–15], acceleration [16–18], and propagation [19–26] of CRs. The AMS-02 measurements of the spectra of the secondary family of nuclei, Li, Be, and B, show that on average their spectra harden above ~ 200 GV by $E^{0.13}$ more than that of the primary family of He, C, and O [27], which indicates that the spectral hardenings may have a propagation origin [28]. Nevertheless, it is shown that the injection hardening scenario can also fit the data reasonably well in a class of propagation models with effective reacceleration of particles in the turbulent medium [29, 30].

∗arXiv: 1909.12857.

© Higher Education Press and Springer-Verlag GmbH Germany, part of Springer Nature 2020

Improved direct measurements of the CR spectra at higher energies are recently available from several experiments. Interestingly, the CREAM [31] and NUCLEON [32] data show hints that the CR spectra become softer for rigidities higher than 10 TV. The precise measurement of the proton spectrum up to 100 TeV by the Dark Matter Particle Explorer (DAMPE) [33, 34] clearly reveal such a spectral softening [35]. On the other hand, ground-based air shower experiemnts show that the all-particle spectrum has a so-called "knee" at energies of a few PeV (e.g., [36–39]). Measurements of the knee of individual composition have relatively large uncertainties [36, 40]. A few measurements of the light composition group, e.g., proton plus helium nuclei, tend to suggest a knee below PeV energies [41]. Most recently, preliminary results about the proton plus helium spectra measured by the HAWC experiment showed also a softening at about 30 TeV energies [42]. Given all these progresses of the measurements, it is thus very interesting to investigate the implications of the wide-band direct and indirect measurements on the CR modeling.

There are some studies based on the data available at different time [45–51]. In particular, several studies propose to account for various spectral structures using multiple populations of CR sources [46–49]. Alternatively, if there are by chance one or a few nearby sources whose contributions are different from the sum of the other background sources, spectral structures may also be produced [52–58]. In light of the new measurements of the CR spectra, in particular, by the DAMPE, we revisit the modeling of CR sources from TeV to 100 PeV in a phenomenological way. Our discussion is within the framework of the above two scenarios, i.e., multiple populations (denoted as model A) and nearby sources (denoted as model B), but with a focus on the $O(10)$ TV spectral features. Both models have good physical motivations. For model A, for example, the remnants of different types of supernovae which are smoothly distributed in the Galactic disk should behave differently in accelerating CR particles. The sum of their contributions can result in complicated spectral features. Alternatively, if the Earth is close to (e.g., $\lesssim 500$ pc) one single accelerator by chance, the distinct spectral feature from this nearby source may naturally give the observed spectral bumps. The purpose of this study is to build an overall model of CRs to describe as many as possible the up-to-date observational data in a wide energy range.

2 Origin of the spectral softening

It is clear that the spectral softenings around ~ 10 TV do not correspond to the PeV knee of CRs, even for A-dependent knees of various compositions. To see this explicitly, we show in Fig. 1 the energy spectra of protons, Helium, protons plus Helium, and the all-particle one, for the fitting with one single component of each species. We assume either an exponential cutoff power-law form or a broken power-law form to describe the spectral softenings of CR nuclei, as

$$\Phi_i(E) = \Phi_{0,i}\left(\frac{E}{\mathrm{TeV}}\right)^{-\gamma_i} \times \exp\left(-\frac{E}{E_{c,i}}\right), \quad (1)$$

and

$$\Phi_i(E) = \Phi_{0,i}\left(\frac{E}{\mathrm{TeV}}\right)^{-\gamma_i} \times \left[1+\left(\frac{E}{E_{b,i}}\right)^{s}\right]^{-\Delta\gamma/s}, \quad (2)$$

where E is the total energy of a particle, the subscription i represents different nuclear species, γ_i is the spectral index below the energy of the softening, $E_{b,i}$ ($E_{c,i}$) is the break (cutoff) energy, s is a smoothness parameter, and $\Delta\gamma$ is the change of the spectral index above $E_{b,i}$. These parameters are determined through fitting to the measurements of energy spectra of individual species by ATIC [2], CREAM [31, 59], NUCLEON [32], and DAMPE [35]. For different nuclear species, we assume that the break (cutoff) energy $E_{b,i}$ ($E_{c,i}$) is proportional to either the atomic number Z_i or the mass number A_i, i.e., $E_{b,i} = Z_i\epsilon_b$ or $A_i\epsilon_b$ ($E_{c,i} = Z_i\epsilon_c$ or $A_i\epsilon_c$). For the broken power-law fit, the proton spectrum suggests that $s = 3.0$ and $\Delta\gamma = 0.35$ can describe the spectral softening well. The other parameters are give in Table 1. The results show that the p+He and the all-particle spectra cannot be reproduced in all these fittings, and additional spectral structures between the $O(10)$ TV softening and the knee of CRs are expected (see also Ref. [60]). In the following we discuss two natural scenarios of these spectral structures.

2.1 Multiple populations of CR sources

It has been widely postulated that there are more than one populations of CR sources in the Milky Way. For instance, supernovae of different types may accelerate particles to different maximum energies, giving various spectral features of CRs [46, 49]. Following Ref. [49], we assume that the spectrum of each population is described by an exponential cutoff power-law function of Eq. (1). We further assume that the cutoff energies of different species

Table 1 Spectral parameters of major CR species assuming ~ 10 TV knees.

Species	$\Phi_{0,i}$ ($\mathrm{m^{-2}\cdot s^{-1}\cdot sr^{-1}\cdot TeV^{-1}}$)	γ_i	ϵ_b (TeV)	ϵ_c (TeV)
p	8.79×10^{-2}	2.57	15	120
He	6.20×10^{-2}	2.51	15	120
C	1.05×10^{-2}	2.56	15	120
O	1.35×10^{-2}	2.56	15	120
Ne	4.73×10^{-3}	2.56	15	120
Mg	7.43×10^{-3}	2.56	15	120
Si	8.78×10^{-3}	2.56	15	120
Fe	1.50×10^{-2}	2.56	15	120

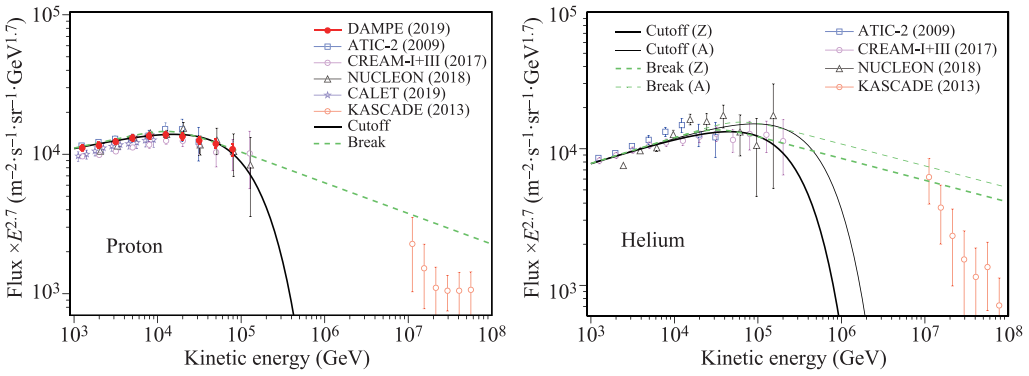


Fig. 1 Energy spectra of protons (top-left), Helium (top-right), proton plus Helium (bottom-left), and all species (bottom-right). In each panel the solid lines show the fitting results with an exponential cutoff form [Eq. (1)], and the dashed lines show the broken power-law [Eq. (2)] fitting results. The thick lines are for the Z-dependent cutoff/break energies, and the thin lines are for the A-dependent cases. References of the data: protons, ATIC [2], CREAM [31], NUCLEON [32], CALET [8], DAMPE [35], KASCADE [43]; Helium, ATIC [2], CREAM [31], NUCLEON [32], KASCADE [43]; p+He, ATIC [2], CREAM [31], ARGO-YBJ [44], ARGO-WFCTA [41]; all-particle, Tibet-III [38], KASCADE [36], GAMMA [39], TUNKA [37].

of each population depend on the atomic number Z_i, i.e., $E_{c,i} = Z_i \epsilon_c$. The fitting results of the major species as well as the all-particle spectrum are shown in Fig. 2. The spectral parameters are summarized in Table 2.

In this scenario, the spectral bumps around 10 TeV are ascribed to the cutoff of population I, with a characteristic cutoff rigidity of ~ 60 TV. The spectra become harder again for rigidities higher than ~ 100 TV, due to the contribution from population II. The cutoff rigidity of population II is about 4 PV, which corresponds to the knee of the all-particle spectrum. We note that the expected spectrum of p+He of this model should also show bump-like feature as that seen in the spectra of protons and Helium. The data from CREAM do show hints of this kind of feature [31]. The preliminary result about the p+He spectrum by HAWC also shows the bump feature at ~ 30 TeV [42], consistent with the model fittings in this work. However, the ARGO-WFCTA data show that the knee of the p+He spectrum is around 700 TeV, which is lower than the 4–8 PeV obtained in our fittings. This is because we

Table 2 Spectral parameters of model A.

Species	Pop. I			Pop. II		
	$\Phi_{0,i}$ ($\mathrm{m^{-2}\cdot s^{-1}\cdot sr^{-1}\cdot TeV^{-1}}$)	γ_i	ϵ_c (TeV)	$\Phi_{0,i}$ ($\mathrm{m^{-2}\cdot s^{-1}\cdot sr^{-1}\cdot TeV^{-1}}$)	γ_i	ϵ_c (TeV)
p	7.78×10^{-2}	2.60	56	1.15×10^{-2}	2.33	4.0×10^3
He	5.84×10^{-2}	2.51	56	6.30×10^{-3}	2.30	4.0×10^3
C	9.92×10^{-3}	2.50	56	7.00×10^{-4}	2.30	4.0×10^3
O	1.66×10^{-2}	2.50	56	1.10×10^{-3}	2.30	4.0×10^3
Ne	2.40×10^{-3}	2.50	56	1.37×10^{-4}	2.30	4.0×10^3
Mg	3.52×10^{-3}	2.50	56	2.22×10^{-4}	2.30	4.0×10^3
Si	6.08×10^{-3}	2.50	56	3.71×10^{-4}	2.30	4.0×10^3
Fe	7.78×10^{-3}	2.37	56	2.27×10^{-3}	2.30	4.0×10^3

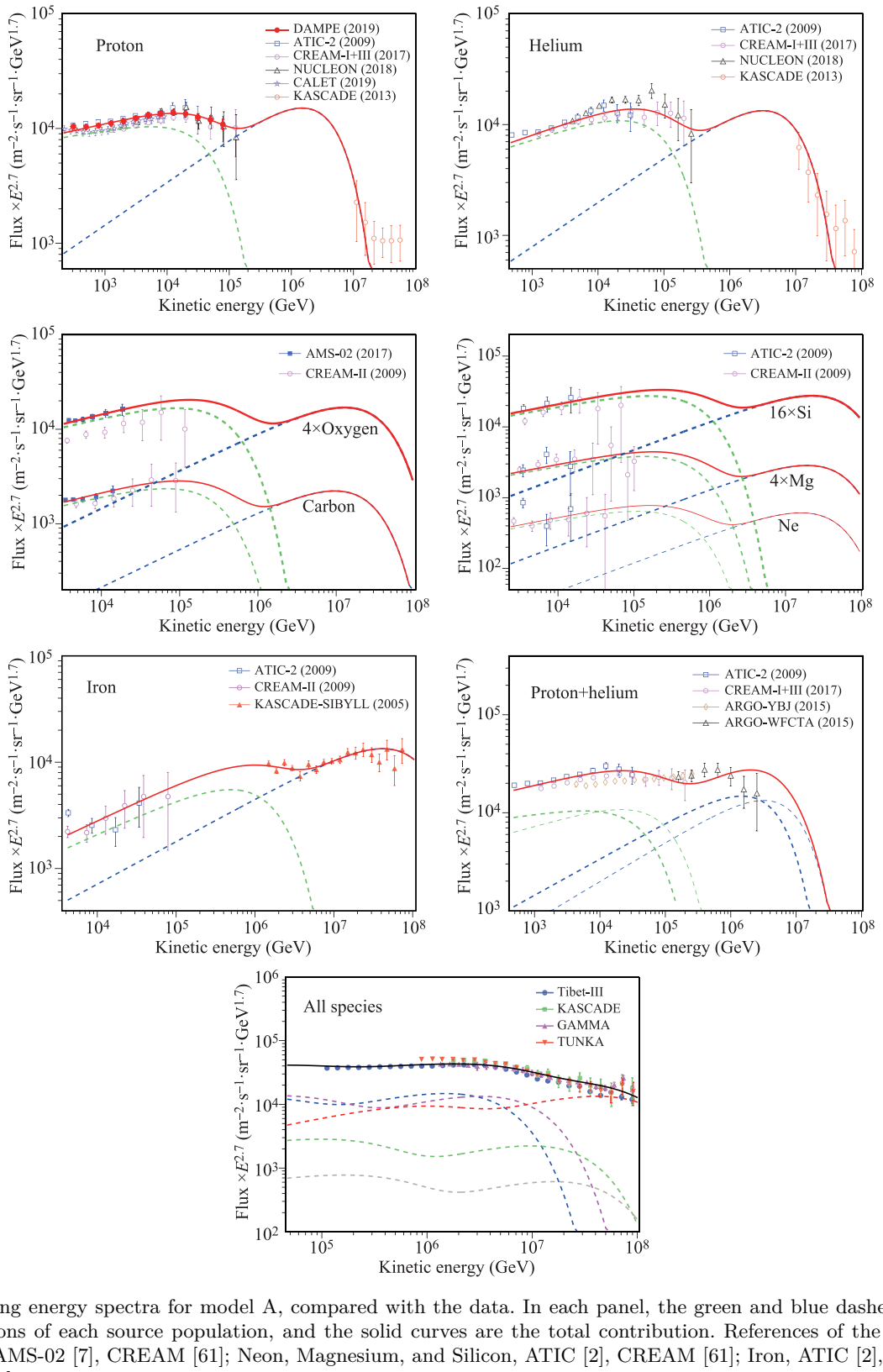


Fig. 2 Fitting energy spectra for model A, compared with the data. In each panel, the green and blue dashed curves show the contributions of each source population, and the solid curves are the total contribution. References of the data: Carbon and Oxygen, AMS-02 [7], CREAM [61]; Neon, Magnesium, and Silicon, ATIC [2], CREAM [61]; Iron, ATIC [2], CREAM [61], KASCADE [36]. The other references are the same as in Fig. 1.

use the KASCADE measurements to determine the cutoff energy of population II. As shown in Ref. [51], the fitting to KASCADE data does favor a higher cutoff energy than the fitting to ARGO data. Improved measurements of the p+He spectra above 100 TeV energies are necessary to understand this slight tension.

2.2 Nearby source(s)

The other scenario to ascribe these spectral features to the contribution of nearby source(s). We assume that the majorities of the observed CR fluxes are due to a background component from the population of sources, and a nearby source component contributes to the $\sim$ 10 TV spectral bumps. The energy spectra of both the background and the nearby components are assumed to be exponentially cutoff power-law functions. The fitting results are shown in Fig. 3, with best-fit parameters compiled in Table 3. For the nearby source, the spectral index is about 2.1 and the cutoff rigidity is about 20 TV. Note that in Ref. [55] a slightly higher cutoff rigidity of $\sim$ 70 TV was derived to

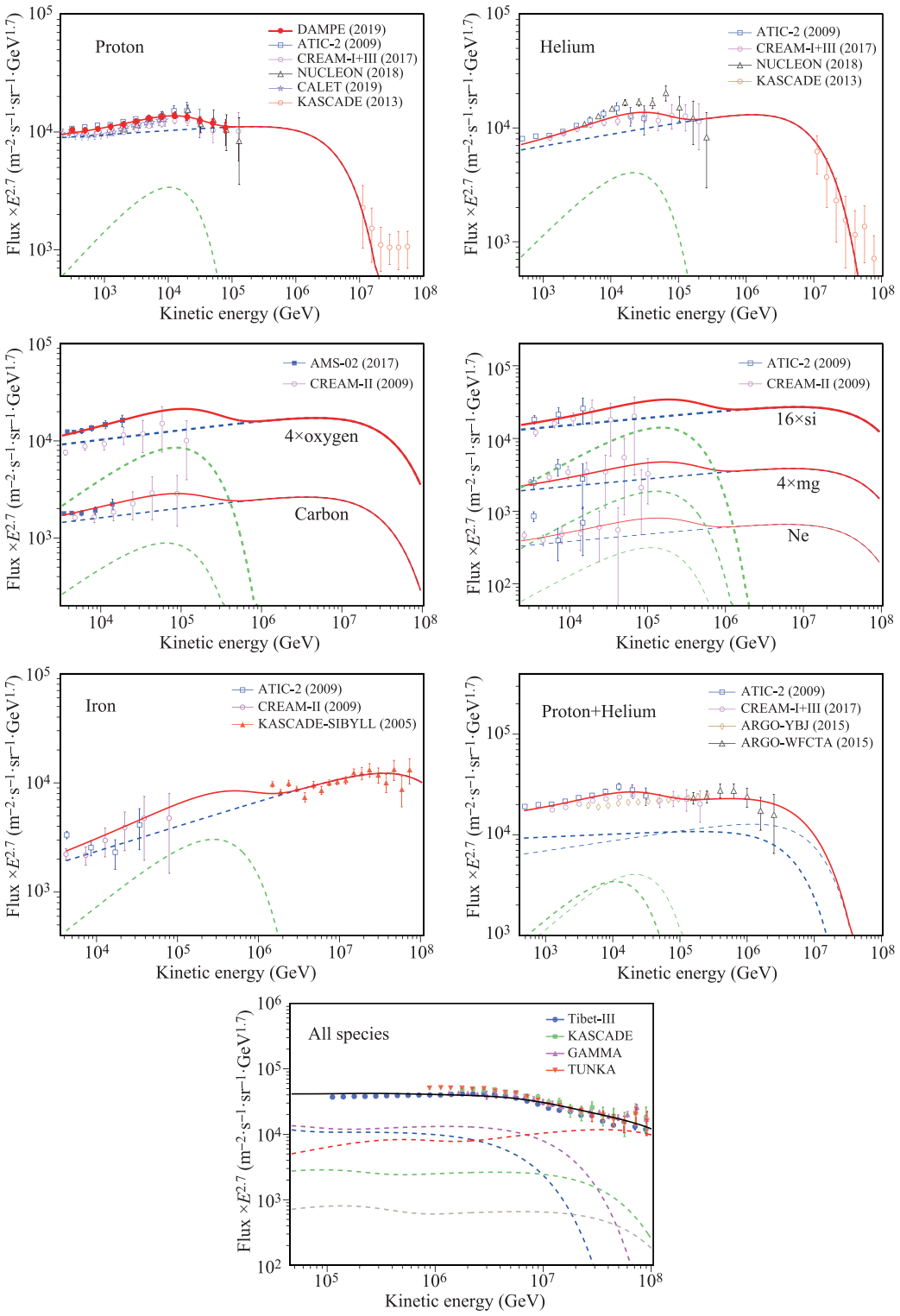


Fig. 3 Same as Fig. 2 but for model B.

Table 3 Spectral parameters of model B.

Species	Background			Nearby source		
	$\Phi_{0,i}$ ($m^{-2}\cdot s^{-1}\cdot sr^{-1}\cdot TeV^{-1}$)	γ_i	ϵ_c (TeV)	$\Phi_{0,i}$ ($m^{-2}\cdot s^{-1}\cdot sr^{-1}\cdot TeV^{-1}$)	γ_i	ϵ_c (TeV)
p	7.41×10^{-2}	2.66	6.0×10^3	1.18×10^{-2}	2.10	18
He	5.55×10^{-2}	2.60	6.0×10^3	9.30×10^{-3}	2.10	18
C	1.02×10^{-2}	2.60	6.0×10^3	1.10×10^{-3}	2.10	18
O	1.63×10^{-2}	2.60	6.0×10^3	2.20×10^{-3}	2.10	18
Ne	2.40×10^{-3}	2.60	6.0×10^3	2.64×10^{-4}	2.10	18
Mg	3.52×10^{-3}	2.60	6.0×10^3	4.03×10^{-4}	2.10	18
Si	6.08×10^{-3}	2.60	6.0×10^3	6.37×10^{-4}	2.10	18
Fe	1.16×10^{-2}	2.48	6.0×10^3	1.28×10^{-3}	2.10	18

fit the CREAM data. This difference is probably due to that the DAMPE data is used in the fit here, and we neglect the CR propagation in this work. This nearby source model (model B) gives comparable goodness-of-fit to the current data, compared with model A described in Sec. III A. These two models may have slight differences in predicting the spectra between 100 TeV and 10 PeV where measurements are lacking. However, we should note that such differences may become smaller through adjusting the model parameters.

Nevertheless, there is a potentially significant difference between models A and B, i.e., the predicted anisotropy pattern of arrival directions of CRs. For model A, the predicted large-scale anisotropies of CRs are the same as the conventional CR diffusion model with a single component of source distribution. The amplitudes of the dipole anisotropies are proportional to E^{δ}, where δ is the energy-dependent slope of the diffusion coefficient. The direction of the anisotropy pattern points from the Galactic center to the anti-center. These model predictions are, however, inconsistent with the measurements of the anisotropies [62–66]. Model B can explain the anisotropy data well [54, 55]. As suggested in Ref. [55], a local source located in the direction that close to Geminga, together with the background source component, can simultaneously explain the spectral features of CR protons and Helium nuclei and the amplitudes and phases of the dipole anisotropies. Specifically, the nearby source dominates the low-energy ($E < 100$ TeV) anisotropies with phases being determined by the direction of the source, and the background dominates the high-energy ($E > 100$ TeV) anisotropies with phases pointing from the Galactic center to the anti-center.

3 Conclusion

Direct measurements of the CR spectra up to 100 TeV by CREAM, NUCLEON, and particularly by DAMPE with high-precision, reveal spectral softenings around ~ 10 TV rigidities. In this work we discuss possible origins of these results, taking into account the wide-band measurements of the CR energy spectra of various mass groups. We show that employing two populations of CR sources with cut-off rigidities of ~ 60 TV and ~ 4 PV can properly fit the measured energy spectra of the main species as well as the all-particle spectrum. Alternatively, including a nearby source on top of the background component gives similar fitting to the spectra. The nearby source model can additionally explain the amplitudes and phases of the large-scale anisotropies of CRs, as long as the source is located at a proper direction in the sky. It has been found that the Geminga supernova remnant may be a promising candidate of such a local source [55].

The revealing of new spectral features of CRs is shown to be able to give very interesting implications on the physics of CRs. The measurement uncertainties of the energy spectra of different mass groups are relatively large for energies higher than 100 TeV, due to the low statistics (for space detection) or the poor composition resolution (for ground-based detection). The under construction Large High Altitude Air Shower Observatory (LHAASO) [67] and the proposed High Energy cosmic-Radiation Detection (HERD) [68] facility onboard the Chinese Space Station are expected to significantly improve the precision of CR spectral measurements. Particularly, the measurements of anisotropies of different mass groups by LHAASO will be essentially helpful in understanding the spectral softening features, the knee structures, and the origin of CRs in general.

Acknowledgements This work was supported by the National Key Research and Development Program of China (No. 2016YFA0400200), the National Natural Science Foundation of China (Nos. 11722328, 11525313, U1738205, and 11851305), and the 100 Talents Program of Chinese Academy of Sciences.

References

1. M. Aguilar, et al., Precision measurement of the boron to carbon flux ratio in cosmic rays from 1.9 GV to 2.6 TV with the alpha magnetic spectrometer on the international space station, *Phys. Rev. Lett.* 117(23), 231102

(2016)

2. A. D. Panov, et al., Energy spectra of abundant nuclei of primary cosmic rays from the data of ATIC-2 experiment: Final results, *Bull. Russ. Acad. Sci. Phys.* 73(5), 564 (2009), arXiv: 1101.3246
3. H. S. Ahn, et al., Discrepant hardening observed in cosmic-ray elemental spectra, *Astrophys. J.* 714(1), L89 (2010), arXiv: 1004.1123
4. O. Adriani, et al., PAMELA measurements of cosmic-ray proton and helium spectra, *Science* 332(6025), 69 (2011), 1103.4055
5. M. Aguilar, et al., Precision measurement of the proton flux in primary cosmic rays from rigidity 1 GV to 1.8 TV with the alpha magnetic spectrometer on the international space station, *Phys. Rev. Lett.* 114(17), 171103 (2015)
6. M. Aguilar, et al., Precision measurement of the helium flux in primary cosmic rays of rigidities 1.9 GV to 3 TV with the alpha magnetic spectrometer on the international space station, *Phys. Rev. Lett.* 115(21), 211101 (2015)
7. M. Aguilar, et al., Observation of the Identical Rigidity Dependence of He, C, and O cosmic rays at high rigidities by the alpha magnetic spectrometer on the international space station, *Phys. Rev. Lett.* 119(25), 251101 (2017)
8. O. Adriani, et al., Direct measurement of the cosmic-ray proton spectrum from 50 GeV to 10 TeV with the calorimetric electron telescope on the international space station, *Phys. Rev. Lett.* 122, 181102 (2019), arXiv: 1905.04229
9. Y. Ohira and K. Ioka, Cosmic-ray helium hardening, *Astrophys. J.* 729(1), L13 (2011), arXiv: 1011.4405
10. Q. Yuan, B. Zhang, and X. J. Bi, Cosmic ray spectral hardening due to dispersion in the source injection spectra, *Phys. Rev. D* 84(4), 043002 (2011), arXiv: 1104.3357
11. A. E. Vladimirov, G. Jóhannesson, I. V. Moskalenko, and T. A. Porter, Testing the origin of high-energy cosmic rays, *Astrophys. J.* 752(1), 68 (2012), arXiv: 1108.1023
12. A. D. Erlykin and A. W. Wolfendale, A new component of cosmic rays? *Astropart. Phys.* 35(7), 449 (2012)
13. S. Thoudam and J. R. Hörandel, Nearby supernova remnants and the cosmic ray spectral hardening at high energies, *Mon. Not. R. Astron. Soc.* 421(2), 1209 (2012), arXiv: 1112.3020
14. G. Bernard, T. Delahaye, Y.-Y. Keum, W. Liu, P. Salati, and R. Taillet, TeV cosmic-ray proton and helium spectra in the myriad model, *Astron. Astrophys.* 555, A48 (2013), arXiv: 1207.4670
15. W. Liu, X.-J. Bi, S.-J. Lin, B.-B. Wang, and P.-F. Yin, Excesses of cosmic ray spectra from a single nearby source, *Phys. Rev. D* 96, 023006 (2017), arXiv: 1611.09118
16. V. Ptuskin, V. Zirakashvili, and E. S. Seo, Spectra of cosmic-ray protons and helium produced in supernova remnants, *Astrophys. J.* 763(1), 47 (2013), arXiv: 1212.0381
17. S. Thoudam and J. R. Hörandel, GeV-TeV cosmic-ray spectral anomaly as due to reacceleration by weak shocks in the galaxy, *Astron. Astrophys.* 567, A33 (2014), arXiv: 1404.3630
18. Y. Zhang, S. Liu, and Q. Yuan, Anomalous distributions of primary cosmic rays as evidence for time-dependent particle acceleration in Supernova remnants, *Astrophys. J. Lett.* 844, L3 (2017), arXiv: 1707.00262
19. N. Tomassetti, Origin of the cosmic-ray spectral hardening, *Astrophys. J.* 752(1), L13 (2012), 1204.4492
20. P. Blasi, E. Amato, and P. D. Serpico, Spectral breaks as a signature of cosmic ray induced turbulence in the galaxy, *Phys. Rev. Lett.* 109(6), 061101 (2012), 1207.3706
21. N. Tomassetti and F. Donato, The connection between the positron fraction anomaly and the spectral features in galactic cosmic-ray hadrons, *Astrophys. J. Lett.* 803, L15 (2015), arXiv: 1502.06150
22. A. M. Taylor and G. Giacinti, Cosmic rays in a galactic breeze, *Phys. Rev. D* 95, 023001 (2017), arXiv: 1607.08862
23. C. Jin, Y. Q. Guo, and H. B. Hu, Spatial dependent diffusion of cosmic rays and the excess of primary electrons derived from high precision measurements by AMS-02, *Chin. Phys. C* 40, 015101 (2016), arXiv: 1504.06903
24. Y. Q. Guo, Z. Tian, and C. Jin, Spatial-dependent propagation of cosmic rays results in spectrum of proton, ratios of p/p, B/C and anisotropy of nuclei, *Astrophys. J.* 819(1), 54 (2016)
25. Y. Q. Guo and Q. Yuan, Understanding the spectral hardenings and radial distribution of galactic cosmic rays and Fermi diffuse gamma-rays with spatially-dependent propagation, *Phys. Rev. D* 97, 063008 (2018), arXiv: 1801.05904
26. W. Liu, Y. H. Yao, and Y. Q. Guo, Revisiting spatial-dependent propagation model with latest observations of cosmic ray nuclei, *Astrophys. J.* 869, 176 (2018), arXiv: 1802.03602
27. M. Aguilar, et al., Observation of new properties of secondary cosmic rays lithium, beryllium, and boron by the alpha magnetic spectrometer on the international space station, *Phys. Rev. Lett.* 120(2), 021101 (2018)
28. Y. Génolini, et al., Indications for a high-rigidity break in the cosmic-ray diffusion coefficient, *Phys. Rev. Lett.* 119, 241101 (2017), arXiv: 1706.09812
29. Q. Yuan, C. R. Zhu, X. J. Bi, and D. M. Wei, Secondary cosmic ray nucleus spectra strongly favor reacceleration of particle transport in the Milky Way, arXiv: 1810.03141 (2018)
30. J. S. Niu, T. Li, and H. F. Xue, Bayesian analysis of the hardening in AMS-02 nuclei spectra, arXiv: 1810.09301 (2018)
31. Y. S. Yoon, et al., Proton and Helium Spectra from the CREAM-III Flight, *Astrophys. J.* 839, 5 (2017), arXiv: 1704.02512
32. E. Atkin, et al., A new universal cosmic-ray knee near the magnetic rigidity 10 TV with the NUCLEON space observatory, *Soviet J. Exp. Theor. Phys. Lett.* 108, 5 (2018), arXiv: 1805.07119

33. J. Chang, Dark matter particle explorer: The first chinese cosmic ray and hard γ-ray detector in space, *Chin. J. Space Sci.* (*Kongjian Kexue Xuebao*) 34, 550 (2014)
34. J. Chang, et al., The Dark matter particle explorer mission, *Astropart. Phys.* 95, 6 (2017), arXiv: 1706.08453
35. Q. An, et al., Measurement of the cosmic-ray proton spectrum from 40 GeV to 100 TeV with the DAMPE satellite, *Sci. Adv.* 5, eaax3793 (2019), arXiv: 1909.12860
36. T. Antoni, et al. (KASCADE Collaboration), KASCADE measurements of energy spectra for elemental groups of cosmic rays: Results and open problems, *Astropart. Phys.* 24, 1 (2005), arXiv: astro-ph/0505413
37. E. E. Korosteleva, V. V. Prosin, L. A. Kuzmichev, and G. Navarra, Measurement of cosmic ray primary energy with the atmospheric Cherenkov light technique in extensive air showers, *Nucl. Phys. B Proc. Suppl.* 165, 74 (2007)
38. M. Amenomori, et al., The all-particle spectrum of primary cosmic rays in the wide energy range from 10^{14} to 10^{17} eV observed with the Tibet-III air-shower array, *Astrophys. J.* 678(2), 1165 (2008), 0801.1803
39. A. P. Garyaka, R. M. Martirosov, S. V. Ter-Antonyan, A. D. Erlykin, N. M. Nikolskaya, Y. A. Gallant, L. W. Jones, and J. Procureur, An all-particle primary energy spectrum in the 3–200 PeV energy range, *J. Phys. G Nucl. Phys.* 35(11), 115201 (2008), 0808.1421
40. M.Amenomori, et al. (Tibet As-gamma Collaboration), Are protons still dominant at the knee of the cosmic-ray energy spectrum? *Phys. Lett. B* 632, 58 (2006), arXiv: astro-ph/0511469
41. B. Bartoli, et al., The knee of the cosmic hydrogen and helium spectrum below 1 PeV measured by ARGO-YBJ and a Cherenkov telescope of LHAASO, *Phys. Rev. D* 92, 092005 (2015), arXiv: 1502.03164
42. J. C. Arteaga-Velazquez and J. D. Alvarez, The spectrum of the light component of TeV cosmic rays measured with HAWC, *Proceedings of Science ICRC* 2019, 176 (2019)
43. W. D. Apel, et al., KASCADE-Grande measurements of energy spectra for elemental groups of cosmic rays, *Astropart. Phys.* 47, 54 (2013)
44. B. Bartoli, et al. (ARGO-YBJ Collaboration), The cosmic ray proton plus helium energy spectrum measured by the ARGO-YBJ experiment in the energy range 3-300 TeV, *Phys. Rev. D* 91, 112017 (2015), arXiv: 1503.07136
45. J. R. Hörandel, On the knee in the energy spectrum of cosmic rays, *Astropart. Phys.* 19, 193 (2003), arXiv: astro-ph/0210453
46. V. I. Zatsepin and N. V. Sokolskaya, Three component model of cosmic ray spectra from 10 GeV to 100 PeV, *Astron. Astrophys.* 458(1), 1 (2006), arXiv: astro-ph/0601475
47. A. M. Hillas, Cosmic rays: Recent progress and some current questions, arXiv: astro-ph/0607109 (2006)
48. T. K. Gaisser, Spectrum of cosmic-ray nucleons, kaon production, and the atmospheric muon charge ratio, *Astropart. Phys.* 35(12), 801 (2012), arXiv: 1111.6675
49. T. K. Gaisser, T. Stanev, and S. Tilav, Cosmic ray energy spectrum from measurements of air showers, *Front. Phys.* 8(6), 748 (2013), arXiv: 1303.3565
50. S. Thoudam, J. P. Rachen, A. van Vliet, A. Achterberg, S. Buitink, H. Falcke, and J. R. Hörandel, Cosmic-ray energy spectrum and composition up to the ankle - the case for a second Galactic component, *Astron. Astrophys.* 595, A33 (2016), arXiv: 1605.03111
51. Y. Q. Guo, and Q. Yuan, On the knee of galactic cosmic rays in light of sub-TeV spectral hardenings, *Chin. Phys. C* 42, 075103 (2018), arXiv: 1701.07136
52. A. D. Erlykin and A. W. Wolfendale, A single source of cosmic rays in the range - eV, *J. Phys. G Nucl. Phys.* 23(8), 979 (1997)
53. L. G. Sveshnikova, O. N. Strelnikova, and V. S. Ptuskin, Spectrum and anisotropy of cosmic rays at TeV–PeV-energies and contribution of nearby sources, *Astropart. Phys.* 50, 33 (2013), 1301.2028
54. V. Savchenko, M. Kachelrieß, and D. V. Semikoz, Imprint of a 2 Myr old source on the cosmic ray anisotropy, *Astrophys. J. Lett.* 809, L23 (2015), arXiv: 1505.02720
55. W. Liu, Y.-Q. Guo, and Q. Yuan, Indication of nearby source signatures of cosmic rays from energy spectra and anisotropies, *J. Cosmol. Astropart. Phys.* 10, 010 (2019), arXiv: 1812.09673
56. X. B. Qu, Understanding the galactic cosmic ray dipole anisotropy with a nearby single source under the spatially-dependent propagation scenario, arXiv: 1901.00249 (2019)
57. B. Q. Qiao, W. Liu, Y. Q. Guo, and Q. Yuan, Anisotropies of different mass compositions of cosmic rays, *J. Cosmol. Astropart. Phys.* 12, 007 (2019), arXiv: 1905.12505
58. D. Karmanov, I. Kovalev, I. Kudryashov, A. Kurganov, V. Latonov, A. Panov, D. Podorozhnyy, and A. Turundaevskiy, A possibility of interpretation of the cosmic ray kneenear 10 TV as a contribution of a single close source, arXiv: 1907.05987 (2019)
59. Y. S. Yoon, et al., Cosmic-ray proton and helium spectra from the first cream flight, *Astrophys. J.* 728(2), 122 (2011), arXiv: 1102.2575
60. P. Lipari and S. Vernetto, The shape of the cosmic ray proton spectrum, arXiv: 1911.01311 (2019)
61. H. S. Ahn, et al., Energy spectra of cosmic-ray nuclei at high energies, *Astrophys. J.* 707(1), 593 (2009), arXiv: 0911.1889
62. M. Aglietta, et al., A measurement of the solar and sidereal cosmic-ray anisotropy at E_0 approximately 10^{14} eV, *Astrophys. J.* 470, 501 (1996)
63. M. Amenomori, et al., Anisotropy and corotation of galactic cosmic rays, *Science* 314(5798), 439 (2006), arXiv: astro-ph/0610671
64. M. Aglietta, et al., Evolution of the cosmic-ray anisotropy above 10^{14} eV, *Astrophys. J.* 692(2), L130 (2009), arXiv: 0901.2740

65. M. G. Aartsen, et al. (IceCube Collaboration), Anisotropy in cosmic-ray arrival directions in the southern hemisphere with six years of data from the IceCube Detector, *Astrophys. J.* 826, 220 (2016), arXiv: 1603.01227

66. M. Amenomori, et al. (Tibet AS-gamma Collaboration), Northern sky galactic cosmic ray anisotropy between 10-1000 TeV with the Tibet air shower array, *Astrophys. J.* 836, 153 (2017), arXiv: 1701.07144

67. X. Bai, et al., The large high altitude air shower observatory (LHAASO) science white paper, arXiv: 1905.02773 (2019)

68. S. N. Zhang, et al. (HERD Collaboration), The high energy cosmic-radiation detection (HERD) facility onboard China's future space station, in: *Proc. SPIE* 9144, 91440X (2014), arXiv: 1407.4866